ARTICLE
Journal of Cellular Biochemistry 109:1274–1285 (2010)

Journal of Cellular Biochemistry

Characterization of Centrosomal Proteins Cep55 and Pericentrin in Intercellular Bridges of Mouse Testes

Yu-Chen Chang,[1,2] Yen-Jung Chen,[3] Chu-Hen Wu,[3,4] Yi-Chen Wu,[3] Tzu-Chen Yen,[2] and Pin Ouyang[3,4,5*]

[1] *Graduate Institute of Clinical Medical Sciences, College of Medicine, Chang Gung University, Tao-Yuan, Taiwan, ROC*
[2] *Department of Nuclear Medicine and Molecular Imaging Center, Chang Gung Memorial Hospital and Chang Gung University, Tao-Yuan, Taiwan, ROC*
[3] *Department of Anatomy, Chang Gung University, Tao-Yuan, Taiwan, ROC*
[4] *Molecular Medicine Research Center, Chang Gung University, Tao-Yuan, Taiwan, ROC*
[5] *Transgenic Mice Core-Lab, Chang Gung University, Tao-Yuan, Taiwan, ROC*

ABSTRACT

Centrosomal protein 55 (Cep55), located in the centrosome in interphase cells and recruited to the midbody during cytokinesis, is essential for completion of cell abscission. Northern blot previously showed that a high level of Cep55 is predominantly expressed in the testis. In the present study, we examined the spatial and temporal expression patterns of Cep55 during mouse testis maturation. We found that Cep55, together with pericentrin, another centrosomal protein, were localized to the intercellular bridges (IBs) interconnecting spermatogenic cells in a syncytium. The IBs were elaborated as a double ring structure formed by an inner ring decorated by Cep55 or pericentrin and an outer ring of mitotic kinesin-like protein 1 (MKLP1) in the male germ cell in early postnatal stages and adulthood. In addition, Cep55 and pericentrin were also localized to the acrosome region and flagellum neck and middle piece in elongated spermatids, respectively. These results suggest that Cep55 and pericentrin are required for the stable bridge between germ cells during spermatogenesis and spermiogenesis. J. Cell. Biochem. 109: 1274–1285, 2010.

KEY WORDS: Cep55; INTERCELLULAR BRIDGE; TESTIS; PERICENTRIN; MKLP1

The centrosome is the principle microtubule organizing center in animal cells, consisting of two main substructures, a pair of centrioles and the pericentriolar material. The centrosome is structurally and functionally regulated in a cell-cycle-dependent manner to form a bipolar spindle that ensures the proper segregation of replicated chromosomes into two daughter cells. The pericentriolar material usually surrounds both centrioles and is the site of microtubule nucleation. In recent years, several studies have identified certain proteins that localize to centrosomes early in mitosis and later to the midbody and are required for cell cleavage, providing a link between the centrosome and cytokinesis [Mishima et al., 2002; Saint and Somers, 2003; Somers and Saint, 2003; Doxsey et al., 2005; Gromley et al., 2005].

Cytokinesis, the division of a cell, involves selection of cleavage plane, rearrangement of microtubule structures, contractile ring assembly, ring ingression, and abscission [Glotzer, 2001; Eggert et al., 2006]. Abscission requires the scission of a thin bridge of membrane connecting the daughter cells. The site of abscission is the midbody, which consists of tightly overlapped anti-parallel non-kinetochore microtubules in a small region located at the spindle equator during the terminal phase of anaphase B [Mullins and Biesele, 1977; Rattner, 1992]. This rigid and unvaryingly sized structure, sometimes called the Flemming body, is a phase-dense circular complex structure that contains proteins required for cell cleavage [Canman and Wells, 2004; Eggert et al., 2006]. With the progression of cytokinesis, the midbody coincides with the position of the cleavage furrow and subsequently positions at the midpoint of a narrow, tubular intercellular bridge (IB) which connects dividing cells. Transient IBs are seen before the completion of cytokinesis in mammal cells [Mullins and Biesele, 1973; Fabbro et al., 2005;

Grant sponsor: Chang Gung Memorial Hospital; Grant number: CMRPD170072; Grant sponsor: Tope Center Grant of Ministry of Education; Grant number: EMRPD180111; Grant sponsor: National Science Council, ROC; Grant numbers: NSC95-2320-B-182-040-MY3, NSC98-2320-B-182-019-MY3.
*Correspondence to: Prof. Pin Ouyang, PhD, Department of Anatomy, Chang Gung University, 259 Wen-Hwa 1st Road, Kwei-Shan, Tao-Yuan, Taiwan 333, ROC. E-mail: ouyang@mail.cgu.edu.tw
Received 24 November 2009; Accepted 5 January 2010 • DOI 10.1002/jcb.22517 • © 2010 Wiley-Liss, Inc.
Published online 23 February 2010 in Wiley InterScience (www.interscience.wiley.com).

Gromley et al., 2005]. The midbody of the dividing cells is discarded asymmetrically into one daughter cell after abscission where it gradually loses its ubiquitin modification and finally disappears [Gromley et al., 2005; Pohl and Jentsch, 2008]. Several organisms, such as plants, fungi, *Caenorhabditis elegans*, and *Drosophila*, however, use stable somatic IBs as cytoplasmic connections [Robinson and Cooley, 1996].

Recently, a striking feature of conversion of the midbody matrix proteins into stable germ cell IBs has been reported [Greenbaum et al., 2007]. The immature male germ cells within seminiferous tubules of murine testes go through a complex series of differentiation involving mitotic and meiotic divisions and finally a series of morphological transformations leading to the formation of mature spermatozoa. Following the breakdown of the midbody and central spindle, stable IBs are observed in mammal germ cells without abscission at the terminal stage of cytokinesis [Burgos and Fawcett, 1955; Fawcett et al., 1959; Dym and Fawcett, 1971; Weber and Russell, 1987]. Only the most primitive spermatogonia complete their cytoplasmic divisions and all other daughter cells are linked through their cytoplasms in syncytia by incomplete cytokinesis and undergo a series of synchronous differentiation steps that culminate in the production of mature sperm. The exact mechanism by which the midbody is converted to IBs and the molecular components involved are still elusive.

Using bioinformatics approaches to screen for novel genes involved in mitosis, over the past few years several groups have independently identified a novel coiled-coil protein, centrosomal protein 55 kDa (Cep55), also named FLJ10540 or C10orf3 [Doxsey, 2005; Fabbro et al., 2005; Martinez-Garay et al., 2006; Zhao et al., 2006; Montoya, 2007; Morita et al., 2007]. Cep55, located on chromosome 10q23.33, encodes a 464-amino acid protein containing three central coiled-coil domains and has been found highly expressed in certain human tumors such as hepatocellular carcinoma and colon cancer [Sakai et al., 2006; Chen et al., 2007]. Western blot analysis of synchronized HeLa cells detected a Cep55 doublet, indicative of phosphorylation during mitosis, and a single protein in interphase cells [Fabbro et al., 2005]. Cep55 was localized to centrosome during mitosis but could be translocated to the midbody and regulated cell abscission during cytokinesis [Fabbro et al., 2005; Martinez-Garay et al., 2006; Zhao et al., 2006]. Cep55 directly associated with the centralspindlin complex in vivo and was under the control of centralspindlin as knockdown of MKLP1 (a component of centralspindlin complex) abolished the localization of Cep55 to the spindle midzone and the midbody [Zhao et al., 2006].

Among the tissues examined by Northern blotting, testis displayed the highest Cep55 expression level while other tissues showed little or minimal expression [Fabbro et al., 2005; Martinez-Garay et al., 2006]. It is therefore intriguing to explore the subcellular localization and function of testicular Cep55 during germ cell formation and development. In this study, we generated antibodies against Cep55 to assess the temporal expression profiles and cellular localization of Cep55 in neonatal and adult mouse testes. The distribution of pericentrin [Doxsey et al., 1994], another conserved centrosomal protein in murine testes, was also studied. We compared the Cep55 and pericentrin expression patterns to a known germ cell bridge marker, MKLP1/CHO1/Pavarotti/ZEN4 [Carmena et al., 1998; Minestrini et al., 2002], first identified as a component of germ cell IBs of *Drosophila melanogaster*, and characterized the subcellular distribution of Cep55 during testicular development. Our results demonstrate for the first time from a morphological point of view that Cep55 and pericentrin, although both being centrosomal proteins, are not only located in the germ cell IBs but also appear inside the ring structure of the IB and form a double ring complex with MKLP1.

MATERIALS AND METHODS

ANTIBODY PRODUCTION

To generate antibodies against Cep55 proteins, we produced bacterially expressed recombinant proteins. The immunogen for monoclonal antibody (mAb) 11A5 was produced by ligating full-length human Cep55 cDNA to the pGEX4T3 vector (Pharmacia Biotech, Uppsala, Sweden) and that for mAb 6A6 was produced by ligating the *Bam*HI–*Sal*I fragment of humanCep55 cDNA (deletion of first 190 amino acids) to the same vector. Both plasmids were transformed into DH5a cells which were then induced with 0.1 mM IPTG for 3 h at 37°C. Purifications of expressed proteins were accomplished by absorption of fusion proteins from bacterial cell lysate to glutathione sepharose 4B followed by elution with 5 mM glutathione in 50 mM Tris–HCl, pH 8.0. For mAb production, 100 mg immunogen was mixed with complete Freunds adjuvant to inject Balb/C mice. Subsequent to three or four booster injections, at 2-week intervals, mice were sacrificed and splenocytes were fused with NS1 myeloma cells. Hybridoma cells grown in HAT-containing RPMI medium were plated into 24-well dishes. Supernatants were screened by immunofluorescence microscopy of HeLa cells cultured on coverslips and Western blot using whole cell protein extracts. Cells of positive wells were selected and cloned by limited dilution.

NORTHERN BLOT ANALYSIS

Total RNA was prepared from the multiple tissues with TRIZOL (Invitrogen, California). Twenty micrograms of total RNA of each tissue was separated by electrophoresis in a 1.2% formaldehyde agarose gel and blotted onto nylon paper. The blots with RNA from multiple mouse tissues were pre-hybridized in 50% formamide, 5× SSC, 5× Denhardt's solution, 0.2% SDS plus 250 μg/ml herring testis DNA for 12 h at 42°C. A ^{32}P-labeled DNA probe consisting of nucleotides 1101–1791 of the full-length murine cep55 cDNA was used for the detection of Cep55 message expression profile. Hybridization was carried out with the labeled probes at 42°C for 12 h. Blots were washed twice at room temperature, 42°C, and 55°C with 2× SSC and 0.1% SDS, each for 15 min, then washed with 0.2× SSC and 0.1% SDS for 30 min, followed by exposure to X-ray films at −80°C with an intensifying screen for 1–12 days. Quantification of signal intensity was carried out with Image J software (NIH, USA) and normalized to that of β-actin RNA.

WESTERN BLOT ANALYSIS

Whole cell extracts of multiple mouse tissues or mouse testes at different developmental stages were prepared by lysing cells in high salt lysis buffer (50 mM Tris–HCl, pH 8.3, 5 mM EDTA, 500 mM NaCl)

containing 1 mM PMSF and 1 mg/ml each of pepstatin, leupeptin, and chemostatin. Samples were sonicated for 30 s on ice and boiled for 5 min prior to electrophoresis on a 10% polyacrylamide gel. In Figure 1C, each lane was loaded with the same amount of total protein lysate (100 μg) from different culture cell lines. Proteins were transferred from the gel to a nitrocellulose paper which was blocked with 5% non-fat dried milk in PBS followed by washing in PBS. Primary antibody incubations, including mouse anti-Cep55 11A5, mouse anti-β-actin (1:2,000, Sigma) were carried out for 1 h at room temperature. After extensive washing in PBS, the paper was incubated for 1 h with HRP-conjugated goat anti-mouse IgG (diluted 1:4,000 in PBS, Jackson Laboratory, West Grove, PA). The peroxidase-labeled blots were developed with an ECL kit (Amersham Biotech, Uppsala, Sweden). Protein amount was quantified with NIH Image J software.

CELL CULTURE AND SYNCHRONIZATION

Human pancreatic cancer cell line MIA Paca 2, PANC-1; human colon cancer cell lines CoLo 205, SW480, SW620; human hepatic cancer cell lines Hep 3B, Hep G2, SK-Hep-1; human breast cancer cell lines MCF7, MDA-MB-4355; human leukemia cell line Jurkat T; human epidermoid carcinoma cell line A431; human lung adenocarcinoma cell lines CL1-0, CL1-5; human cervical cancer cell lines HeLa, C33A; human nasopharyngeal carcinoma cell lines NPC-BM1, NPC-TW02, NPC-TW04; human oral cancer cell lines OEC-M1, SCC-4; human bladder tumor cell lines U1, U4; and human neuroblastoma cell line SKNSH of passages 10–30 were maintained in DMEM/F12 (Gibco/Invitrogen, California) supplemented with 10% fetal bovine serum (FBS, Gibco/Invitrogen), 2 mM glutamine, and 200 U/ml each of streptomycin and penicillin G. Cells were passed with 0.1% trypsin and 0.04% EDTA in Hank's medium.

To obtain synchronized cells, HeLa cells were grown in a T75 flask to 70–80% confluency and then exposed to 3 μg/ml nocodazole (Sigma) for 22 h to arrest cells at metaphase [Terasima and Tolmach, 1963]. After the drug was carefully washed out from the culture, cells were collected by mitotic shake-off [Tobey et al., 1967] and incubated further in fresh medium at 37°C. To observe cells at different stages of mitotic progression, acetone treatment followed by immunostaining was performed at different time points within a 2–8 h period.

IMMUNOHISTOCHEMISTRY

Five micrometer sections of mouse testis tissues were cut from the 4% paraformaldehyde-fixed and paraffin-embedded specimens. Briefly, the sections were deparaffinized in xylene for 5 min four times and rehydrated in serial dilutions of ethanol (100%, 95%, and 75%) for 5 min each. Antigen retrieval was performed by placing slides in 1× Rodent Decloaker (Biocare Medical, Inc., Concord, CA) and heating to 95°C for 30 min using a rice cooker. The slides were washed with distilled water for 1 min once and then with TBS for 5 min twice. The sections were incubated overnight at 4°C with rabbit anti-Cep55 antibody (1:100, Aviva Systems Biology, San Diego, CA). After 13 h, the slides were washed with TBS and then incubated for 30 min at room temperature with secondary antibody Rabbit on Rodent AP-Polymer (Biocare Medical, Inc.). Vulcan Fast Red Chromogen Kit2 (Biocare Medical, Inc.) was employed in the detection procedure. The slides were counterstained with hematoxylin for 5 min, washed, dehydrated, and coverslipped.

PREPARATION OF ENZYME-DISSOCIATED TESTICULAR CELLS

The testes of BALB/C mice were used for experiments. The testes were collected in PBS, and the tunica albunigea was removed with sterile forceps and discarded. The tissues were minced into small blocks and seminiferous tubules were dissociated by enzymatic digestion with 0.05–0.1% collagenase type IV (Worthington Biochemical Corporation, Lakewood, NJ) and 0.05% hyaluronidase (Worthington Biochemical Corporation) for 15 min in a shaking water bath (100 cycles/min) at 30°C. The cells were washed twice with PBS and the resulting whole cell suspension was filtered through a 40 mm nylon mesh to remove cell clumps. Dissociated cells were washed by PBS and fixed for 15 min with 0.5% paraformaldehyde. Cell concentrations were estimated with a hemocytometer and $\sim 6 \times 10^4$ cells were air-dried on polylysine-coated slides.

IMMUNOFLUORESCENCE MICROSCOPY

Sample slides obtained from culture cells, enzyme-dissociated testicular cells, or testis tissues embedded in OCT and snap frozen were fixed with 0.5% paraformaldehyde for 10 min. Following PBS washing, the slides were incubated in 1% TritonX-100 for 10 min at room temperature to permeabilize the membranes and increase antibody access. After permeabilization, the slides were washed with PBS and blocked in 10% normal goat or donkey serum for 1 h. For primary antibody staining, the slides were incubated with mAb 11A5 or 1:200 rabbit anti-Cep55 antibody (Aviva Systems Biology), 1: 500 rabbit anti-pericentrin antibody (Abcam), or 1:200 goat anti-MKLP-1 antibody (Santa Cruz) overnight at 4°C. Following washing with PBS, the slides were incubated with secondary immunoreagents including Fluorescein (FITC)-conjugated donkey anti-goat IgG (Jackson Laboratory) at 1:100 dilution, Alexa Fluor 594-conjugated donkey anti-mouse IgG, Alexa Fluor 488-conjugated donkey anti-rabbit IgG, and Alexa Fluor 594-conjugated donkey anti-goat IgG (Invitrogen) at 1:500 dilution for 1 h. Finally, the slides were washed with PBS and mounted with mounting medium (50% glycerol and 0.4% *n*-propylgallate) containing DAPI for nuclear staining, and examined with a photomicroscope (Carl Zeiss, Germany) equipped with epifluorescence.

RESULTS

CHARACTERIZATION OF MONOCLONAL ANTI-Cep55 ANTIBODIES

As the first step toward characterizing Cep55 proteins in murine tissues, we generated antibodies against murine Cep55 proteins. mAbs 11A5 and 6A6 were raised against the full-length and C-terminal (191–464 amino acids) sequences of Cep55, respectively (Fig. 1A). The specificity of antibodies was demonstrated by Western blot analysis of cell lysates prepared from *E. coli* that had been transformed with GST-fused full length, C-terminal truncated (Δ191–464 amino acids), or N-terminal truncated (Δ1–190 amino acids) Cep55 cDNAs (Fig. 1B). The lysates were separated by SDS–PAGE and either stained with Coomassie Brilliant Blue to identify the expressed proteins or probed with mAb 11A5 or 6A6. Both mAbs

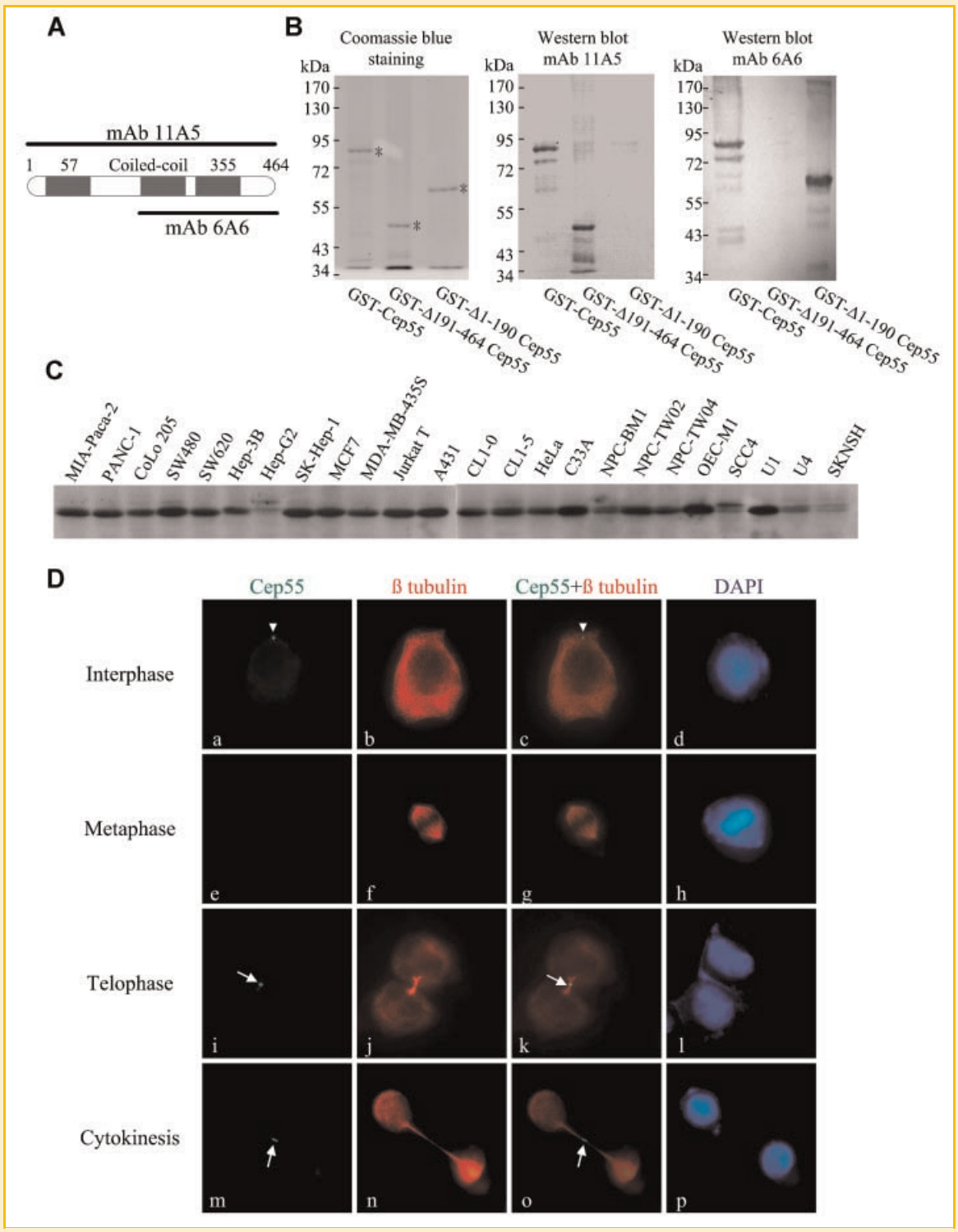

Fig. 1. Characterization of Cep55 monoclonal antibodies (mAbs). A: Schematic representation of the locations of the immunogens used to generate mAbs 11A5 and 6A6. Numbers depict the amino acid in length at Cep55. Filled rectangles denote coiled-coil domain. B: Immunoreactivity of GST-Cep55 fusion proteins with mAbs 11A5 and 6A6. Total protein lysates prepared from *E. coli* transformed with various GST-Cep55 constructs were separated by SDS–PAGE and stained with Coomassie Brilliant Blue. GST fusion proteins were expressed and observed as major bands (*, left panel). MAb 11A5 recognized full-length and C-terminus deleted fusion proteins (middle panel), while mAb 6A6 decorated, on the contrary, full-length and N-terminus deleted fusion proteins (right panel) upon Western blotting. C: Immunoblotting analysis of different tumor cell lines expressing Cep55 using mAb 11A5. Each lane was loaded with the same amount of total protein lysate. D: Cep55 is expressed at centrosomes and midbody during cell-cycle progression. HeLa cells were treated with nocodazole for 22 h and relieved for 2–8 h. Cells were stained with mAb 11A5 (green) and antibody against β-tubulin (red), and DNA was visualized with DAPI (blue). Cep55 is expressed in the centrosome (arrowheads in a and c) in interphase and at midbody (arrows in i, k, m, and o) during cell-cycle progression but not associated with spindle pole in the metaphase (e–g). [Color figure can be viewed in the online issue, which is available at www.interscience.wiley.com.]

11A5 and 6A6 recognized full-length GST fused-Cep55 (Fig. 1B, lane 1 of middle and right panels). Nevertheless, mAb 11A5 (Fig. 1B, lane 2, middle panel) recognized Cep55 N-terminal 1–190 aa but not the C-terminal fragment, and vice versa for mAb 6A6 (Fig. 1B, lane 3, right panel), indicating differential epitope recognition by each antibody. To confirm the ability of our mAb recognized endogenous Cep55, we compared the expression levels of Cep55 proteins in 24 tumor cell lines detected by Western blot (Fig. 1C). Cep55 proteins were highly or moderately expressed in all human cancer cell lines tested with exception of Hep G2 and SKNSH cells, consistent with the suggestion that levels of Cep55 correlated positively with cell proliferation [Chen et al., 2007]. To determine the subcellular localization of endogenous Cep55 proteins, we next used synchronized HeLa cells and performed double immunostaining with mAb 11A5 against Cep55 and β-tubulin antibody (Fig. 1D). For cells in interphase, Cep55 was localized to the microtubule-organizing center (MTOC) (arrowheads in Fig. 1D,a,c) adjacent to the nucleus, suggesting that 11A5 decorates Cep55 at the centrosome. In metaphase cells, however, there was no detectable Cep55 signal within the cytoplasm (Fig. 1D,e–h). These results contrast with those of Martinez-Garay et al. [2006] who observed Cep55 at the spindle pole during metaphase, but are consistent with the report by Fabbro et al. [2005]. This discrepancy was probably due to antibody specificity. Subsequent to cell division, Cep55 was observed accumulating at the cleavage furrow (arrows in Fig. 1D,i–l) and midbody (arrows in Fig. 1D,m–o) at telophase and during cell abscission, respectively. Taken together, we generated Cep55 monospecific antibodies which recognized not only different epitopes but also detected Cep55 at various subcellular locations including centrosomes and midbody during cell-cycle progression.

EXPRESSION ANALYSIS OF Cep55 IN DEVELOPING AND ADULT TESTES

Previous studies showed that Cep55 mRNA was highly expressed in testis and thymus and expressed weakly in colon, small intestine, ovary, and placenta based on Northern blotting [Fabbro et al., 2005; Martinez-Garay et al., 2006]. In order to get a picture of Cep55 protein expression patterns, we performed Western blot analysis with protein samples from multiple tissues of mice (Fig. 2A). The Cep55 protein is expressed highly in testis, weakly in kidney, liver, and thymus, and with little to no expression in other tissues examined, indicating that expression of Cep55 proteins, like that of its messages, was tissue-specific.

To comprehend fully the expression patterns of Cep55 in testes, we then investigated the Cep55 messenger RNA (mRNA) and protein expression profiles during the course of pubertal testis development. The Cep55 mRNA expression levels, as detected by Northern blotting, was low up to 18 days postpartum (p18), when the spermatocytes had matured to the late pachytene stage (Fig. 2B, lanes 1 and 2) [Bellve et al., 1977]. However, there was an abrupt increase in the expression of Cep55 transcripts starting at p23 (Fig. 2B, lane 3), when the most mature germ cells were early round spermatids. Cep55 transcripts were highly expressed at p32 (Fig. 2B, lane 4), a period when elongated spermatids could be found, then declined somewhat after spermiation at p37 (Fig. 2B, lane 5). Western blot analysis revealed a low level of Cep55 protein expression in murine testes between p8 and p13 (Fig. 2C, lanes 1 and 2), corresponding to the time when spermatogonia and early primary spermatocytes appeared. The Cep55 proteins reached a peak expression level at p15 (Fig. 2C, lane 3) and then remained at a substantial level up to p42 (Fig. 2C, lanes 4–8). Although the peak Cep55 protein expression was earlier than that of mRNA (Fig. 2D), there was no obvious delay between the onset of mRNA and protein expression of Cep55, suggesting that Cep55 did not behave like a spermatid-specific gene.

LOCALIZATION OF Cep55 TO GERM CELL INTERCELLULAR BRIDGES IN ADULT MURINE TESTES

The above findings suggested that Cep55 was predominantly expressed in testis. These data prompted us to investigate the subcellular distribution and expression patterns of Cep55 during germ cell development in mouse testes. We examined the localization of Cep55 in mouse testis paraffin sections by immunohistochemical techniques using a rabbit anti-Cep55 antibody. Cep55 antibody reaction products were consistently and readily observed around the germ cells lining the outer rim of seminiferous tubules, while marked variation of staining was detected at the adluminal surface along the tubule inner rim (Fig. 3A,B). In general, stage VI–VIII tubules displayed prominent Cep55 staining along the lumen compared to tubules of other stages. Closer examination of the stage VII seminiferous tubule (Fig. 3C–F) revealed that the most intense Cep55 signals were in residual bodies adjacent to step 16 spermatids (Fig. 3F, arrowhead in inset), while strong Cep55 immunoreactivity at the outer rim of tubule represented intercellular dot structures (Fig. 3D, arrow in inset) connecting spermatocytes (the cytoplasm of germ cells were not clearly seen because the sections were counterstained only with hematoxylin). Interestingly, Cep55 immunoreactivity was also observed as a typical ''ring'' structure among round spermatids (Fig. 3E, arrow in inset), which, along with the dot-like staining among spermatocytes (Fig. 3D), were reminiscent of structures representing IBs among germ cells and suggested that Cep55 might participate in the IBs connecting germ cells as a whole.

CO-EXPRESSION OF Cep55 AS WELL AS PERICENTRIN WITH MKLP1 AT GERM CELL INTERCELLULAR BRIDGES IN DEVELOPING AND ADULT TESTES

To confirm that Cep55 was indeed localized to germ cell IBs, we made testes cryosections from developing and adult mice and co-stained Cep55 with a known bridge component, mitotic kinesin-like protein 1 (MKLP1) by double immmunofluorescence microscopy (Fig. 5).

It has been reported that IBs of germ cells can be considered as counterparts for the midbody in somatic cells [Greenbaum et al., 2007] and midbody components are often expressed at centrosomes [Rattner, 1992], we therefore also sought to determine whether other centrosomal proteins, like Cep55, could be found co-expressed with the IB component in testicular cells. Before examining Cep55 and MKLP1 co-localization in testicular cryosections, we compared the subcellular distribution pattern of Cep55 and pericentrin, a well-defined centrosomal protein, to that of MKLP1 in HeLa cells by

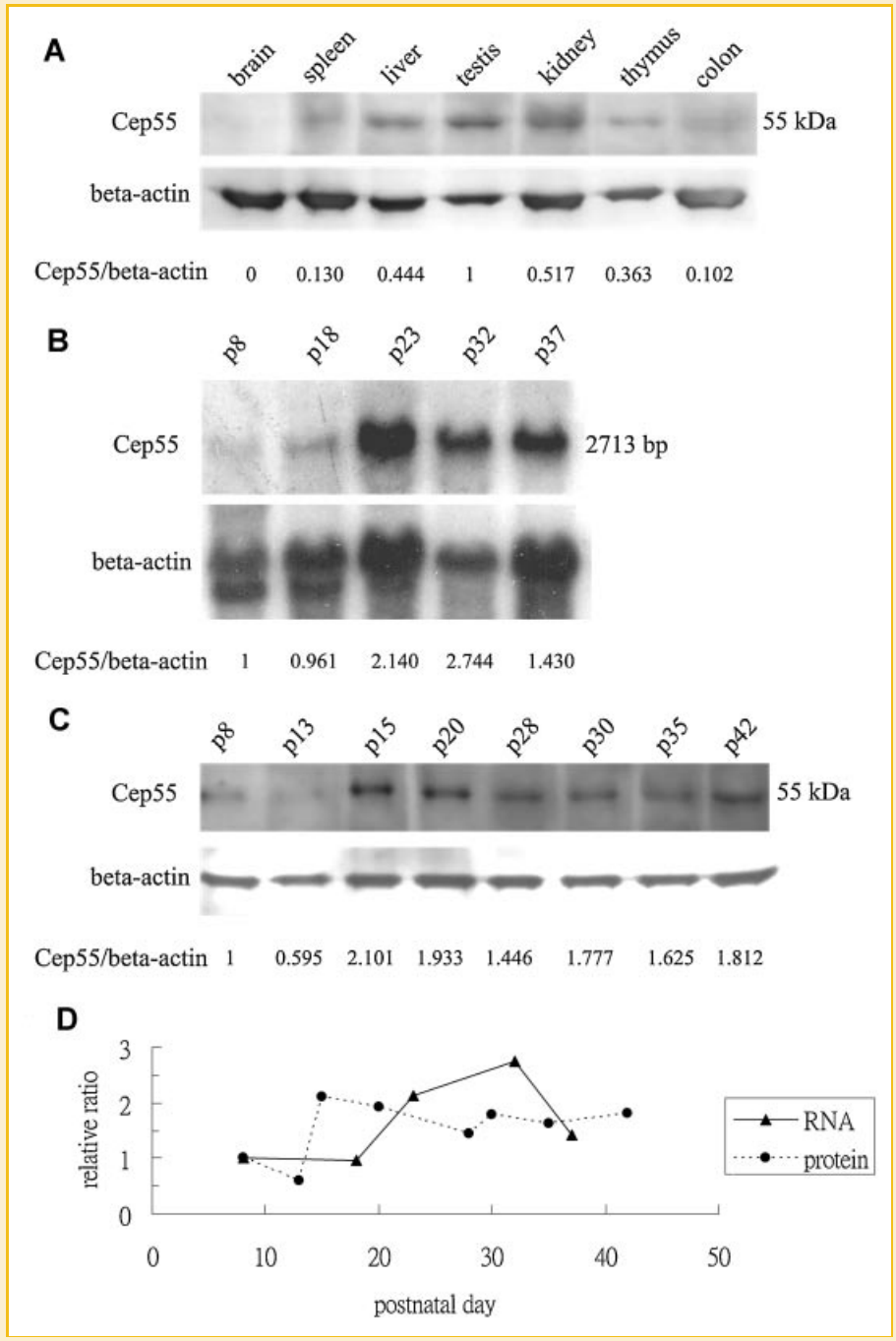

Fig. 2. Expression of Cep55 in adult and developing testes. A: Western blot analysis of Cep55 protein expression in multiple mouse tissues. Among tissues examined, testes showed highest expression levels. β-Actin was used as a loading control. B: Northern blot analysis of Cep55 mRNA expression in mouse developing testes at ages of 8–37 days (p8–p37). β-Actin mRNA was used as a loading control. C: Western blot analysis of Cep55 protein expression in mouse developing testes at different postnatal days (p8–p42). β-Actin was used as a loading control. D: Schematic summary of the expression profiles of Cep55 transcripts and proteins during testis development. The abscissa denotes days postpartum and the ordinate represents fold of expression. day 8 was set as 1.

double immunofluorescence. While MKLP1 could be found at both centrosomes and midbodies (Fig. 4B,E), Cep55 co-localization with MKLP1 was found predominately in the midbody of dividing cells (Fig. 4A–D). Unlike Cep55, pericentrin, though co-localized with MKLP1, was present only in centrosomes, but not in the midbody (Fig. 4E–H). Thus, centrosomal proteins, but not necessarily expressed at midbody, may well co-localize with IB components and assist in IBs between germ cells (see the results below).

Using testicular cryosections from various developing stages, we additionally analyzed the temporal expression patterns of Cep55, pericentrin, and MKLP1 by double immunofluorescence (Fig. 5). At p16, when pachytene spermatocytes appeared, Cep55, as well as

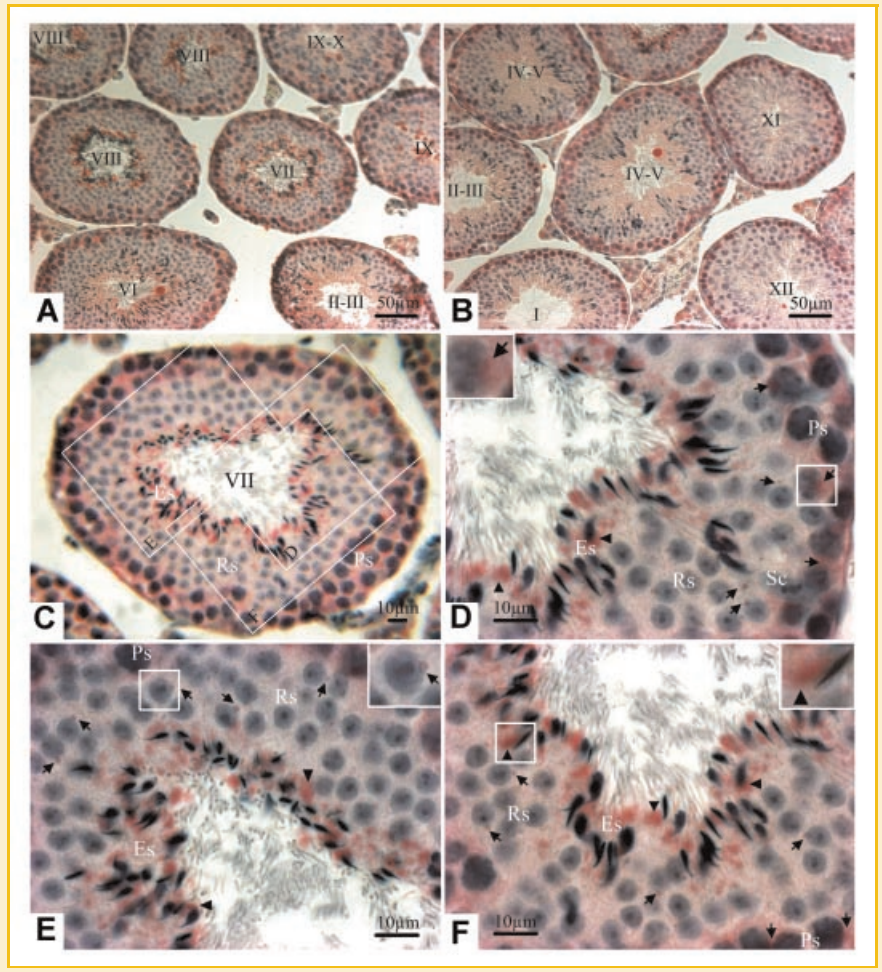

Fig. 3. Immunohistological localization of Cep55 in adult mouse testis. Paraffin sections of mouse testes were immunostained with a polyclonal antibody against Cep55 followed by color developing with alkaline phosphatase and counter stained with hematoxylin. A,B: Lower magnification views of Cep55 immunolocalization at different stages of seminiferous tubules are indicated by roman numerals. C: Cep55 expression in a stage VII seminiferous tubule. The rectangles in (C) corresponded to enlarged views in (D–F). Arrows in (D–F) marked specific Cep55 immunoreactions at primary spermatocytes and round spermatids, while arrowheads marked immunoreactions at elongated spermatids. Insets in (D) and (E) showed a higher magnification of "ring" structure decorated by Cep55 reaction in a primary spermatocyte and in a round spermatid, suggesting the possible involvement of Cep55 in intercellular bridges. Inset in (F) displayed Cep55 immunoreactivity in residual body attached to an elongated spermatid. Ps, spermatocytes; Sc, Sertoli cells; Rs, round spermatids; Es, elongated spermatids. [Color figure can be viewed in the online issue, which is available at www.interscience.wiley.com.]

pericentrin, were expressed with MKLP1 in a unique pattern (Fig. 5A–C,A′–C′) at IBs connecting spermatocytes. Interestingly, it was found that Cep55 and pericentrin formed the central ring of the IBs, while MKLP1 was localized at outer ring surrounding Cep55 and pericentrin (insets, Fig. 5A–C,A′–C′). During the period between p20 and p32, Cep55 and pericentrin co-expressed persistently with MKLP1 as a two-layered structure in the IBs of spermatocytes without significant change (Fig. 5D–L,D′–L′, and insets therein). In adult mouse testes sections, as in developing testes, Cep55 and pericentrin were clearly present in the inner portion of the larger IBs of spermatocytes (insets, Fig. 5M–O,M′–O′), but not detected in the smaller IBs of round spermatids, which can be identified by MKLP1 staining. The reason that Cep55 and pericentrin could not be identified at IBs between round spermatids was probably because of antigen masking in cryosection tissues, which could be resolved by observation of enzymatically dissociated testicular cells (see results below). Immunofluorescent profiling of Cep55 expression patterns from developing mouse testes indicated that Cep55 expression levels increased along with maturation of mouse testes, which was quite consistent with the results of Cep55 protein expression from Western blotting (Fig. 2C), in which Cep55 levels were high after p15 and later stages.

Cep55 AND PERICENTRIN FORM AN INNER RING IN STABLE INTERCELLULAR BRIDGES FROM DISSOCIATED MALE GERM CELLS

To study the localization of Cep55 and pericentrin with regard to IBs in germs cells in more detail, we performed immunofluorescent staining of enzyme-dissociated spermatogenic cells from mouse testes. Both IBs joining spermatocytes and round spermatids contained an inner Cep55 (Fig. 6A–F) or pericentrin (Fig. 6J–O) ring in contrast to MKLP1, which was located at outer ring. In step 15–16 spermatids, Cep55, pericentrin, and MKLP1 positive products were observed within the residual cytoplasm, and were later shed from testicular sperm in residual bodies (Fig. 6G–I,P–R). Cep55

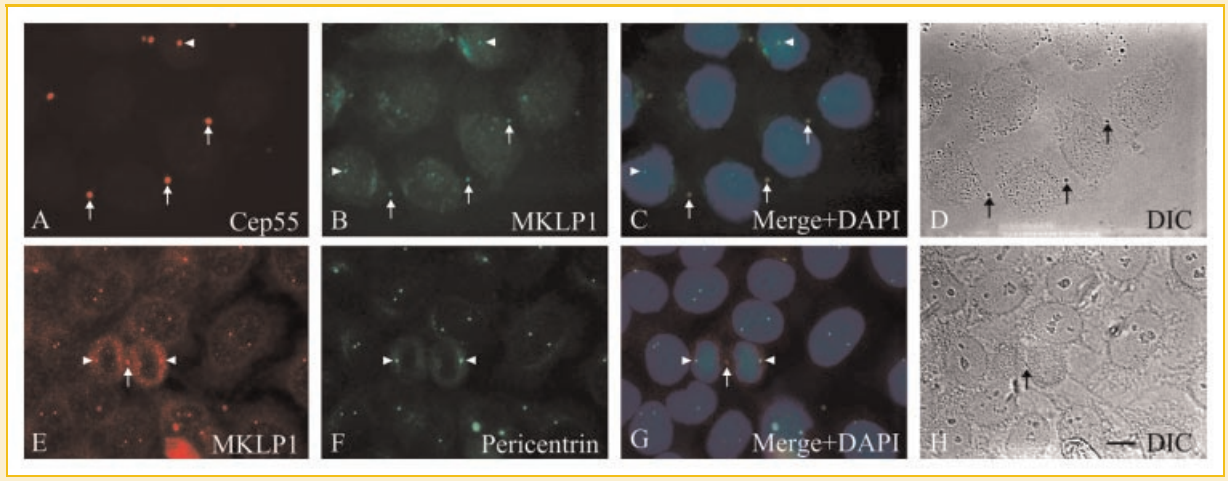

Fig. 4. Subcellular distribution of Cep55, MKLP1, and pericentrin in quiescent and dividing HeLa cells. Double immunofluorescent staining with Cep55 (red) and MKLP1 (green) indicated that Cep55 not only co-localized with MKLP1 at the midbody in dividing cells (arrows, A–D) but at the centrosomes of interphase cells (arrowheads, A–C). Pericentrin (green) was co-localized with MKLP1 (red) at centrosomes (arrowheads, E–G) but not at the midbody (arrows, E, G, and H). Corresponding DIC images (D, H) are shown. Scale bar: 10 μm. [Color figure can be viewed in the online issue, which is available at www.interscience.wiley.com.]

immunofluorescence was also noted in the acrosome region (Fig. 6G) in elongated spermatids or sperms; and pericentrin was found in the neck region and middle piece of the flagellum (Fig. 6P), while MKLP1 was detected in the perinuclear ring and along the whole flagellum (Fig. 6H,Q).

DISCUSSION

Cep55, as reported previously by Northern analysis [Martinez-Garay et al., 2006], was highly expressed in certain human tumors, such as hepatocellular carcinoma [Chen et al., 2007], colon cancer [Sakai et al., 2006], lung cancer [Chen et al., 2009], and head and neck squamous cell carcinoma [Gemenetzidis et al., 2009]. Cep55 has been demonstrated by several laboratories to display dynamic cellular distribution patterns during cell-cycle progression [Fabbro et al., 2005; Martinez-Garay et al., 2006; Zhao et al., 2006]. However, none of these studies was performed with a mAb and their results were variable due to the polyclonal nature of antibodies used. In this study, we generated monospecific antibodies against Cep55 which were harnessed to detect the expression patterns of Cep55 in male germ cells during development of mouse testes. These anti-Cep55 mAbs were used only for Western blot and cultured cell immunofluorescent studies. Based on the expression levels of Cep55 in mice testes from birth to adulthood, we determined the expression profiles of Cep55 transcripts versus proteins during testicular development (Fig. 2). Cep55 expression was barely detectable at the p8–p13 stage but plateaued to a maximum at p15 and subsequently maintained a constant value. Immunocytochemical data confirmed Cep55 expression profiles in developing testes, suggesting a functional role for Cep55 in developing testes. To elucidate the subcellular distribution of Cep55 in developing testes, we also determined the distribution pattern of Cep55 in testicular germ cells. Specifically, we demonstrate here for the first time that Cep55 and pericentrin, both centrosomal proteins, are consistently located within the matrix of the germ cell IBs in neonate to adult mouse testes. In addition to germ cell IBs, Cep55 and pericentrin are distributed in some parts along the elongated spermatids as well as in residual bodies.

Stable germline IBs which are relatively conserved in species ranging from insects [Robinson et al., 1994; Robinson and Cooley, 1996] to mammals [Burgos and Fawcett, 1955; Russell et al., 1987; Weber and Russell, 1987; Greenbaum et al., 2006, 2009] connect both the female and male germline cells in syncytia at least for a period of time during their development. The possible functions of IBs in germ cell development include: (1) to allow genetically segregated haploid spermatids to share diploid gene products after meiosis, (2) to mediate rapid transfer of some vital signals or nutrients, or (3) to eliminate stochastic gene expression which results in a large degree of male germ cell heterogeneity, so that relatively uniform gametes with normal functions can be produced [Guo and Zheng, 2004]. The architecture of the IB is far more complex. In some cell types, such as tissue culture cells of Indian muntjac, seven alternating light and dark zones along the bridge with the midbody at the center are recognized by electron microscopy [Rattner, 1992]. Each zone of the bridge has a characteristic protein composition in which many proteins originate at the same specific site within the cell including spindle microtubules, the interphase nucleus, the metaphase chromosome, and the centrosome [Rattner, 1992]. In addition, the composition of an individual zone may change as the bridge matures [Rattner, 1992; Greenbaum et al., 2007]. However, germ cell cytokinesis initially appears identical to somatic cell cytokinesis observed by electron microscopy with a dense band of amorphous or finely filamentous material, representing the midbody which traverses in the center of the new forming bridge [Burgos and Fawcett, 1955; Fawcett et al., 1959; Dym and Fawcett, 1971; Weber and Russell, 1987]. The traverse midbody subsequently breaks down via an unknown

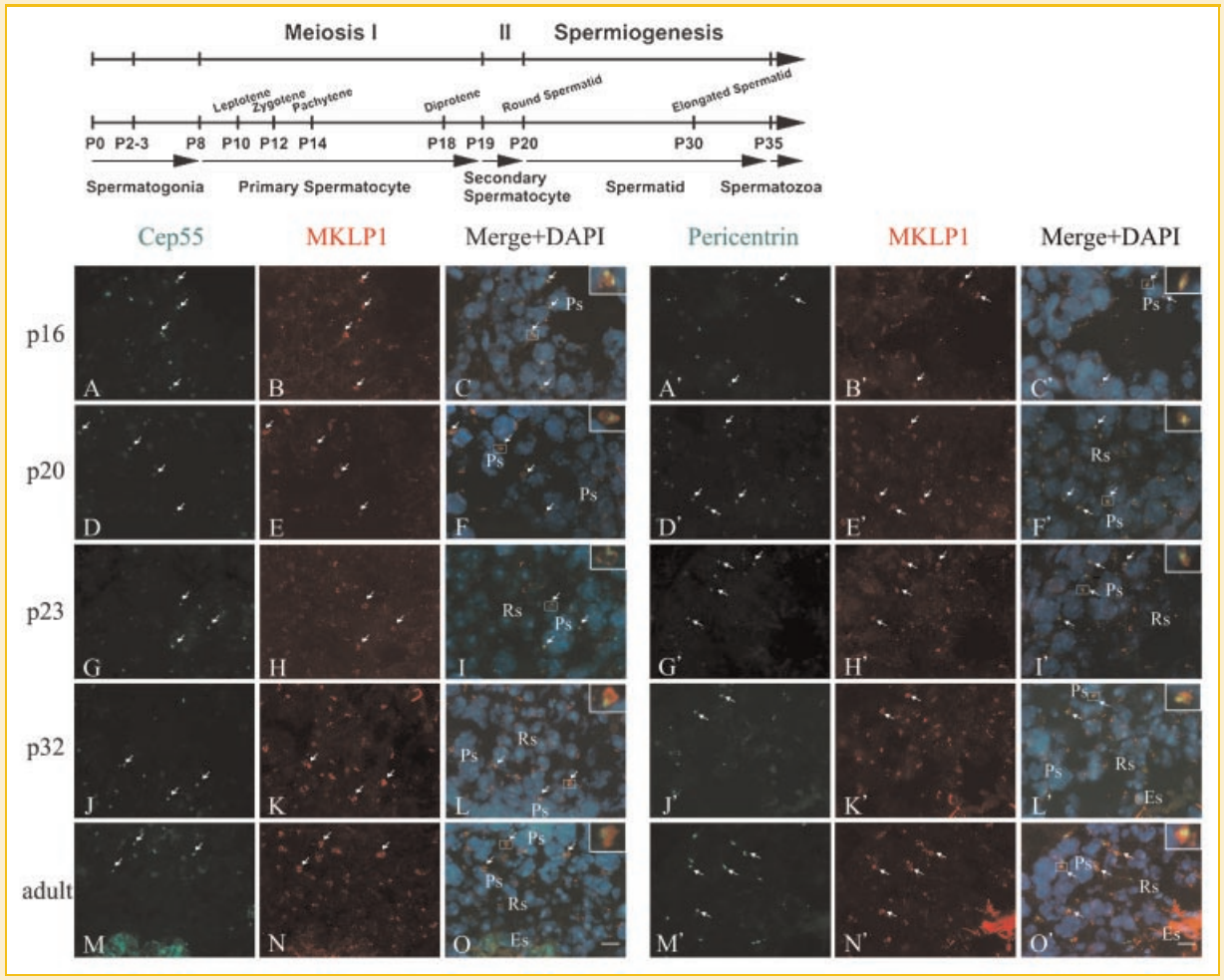

Fig. 5. Subcellular localizations of Cep55, MKLP-1, and pericentrin in mouse testes at different maturation stages to adult. Upper panel shows the time scale for testicular germ cell development in a mouse testis. Lower panel depicts the intercellular bridge localization of Cep55, MKLP1, and pericentrin in mouse testes during development. Double staining with Cep55 (green) and MKLP-1 (red) is depicted in the left column (A–O), and double staining with pericentrin (green) and MKLP-1 (red) is shown in the right column (A′–O′). Arrows indicate co-expression of Cep55 or pericentrin with MKLP1 in intercellular bridges between spermatocytes at each stage. Insets at each merged photo specifically denoted the double ring structure of intercellular bridge outlined by outer MKLP1 staining and inner Cep55 or pericentrin staining. Note that neither Cep55 nor pericentrin can be found in intercellular bridges, as determined by MKLP1 staining, in round spermatids at various stages. The nuclei were counterstained with DAPI (blue signal). Ps, spermatocytes; Rs, round spermatids; Es, elongated spermatids. Scale bar: 10 μm. [Color figure can be viewed in the online issue, which is available at www.interscience.wiley.com.]

mechanism, leaving an electron dense bridge density seen only lining the IB without abscission [Dym and Fawcett, 1971; Weber and Russell, 1987].

Several molecular components of IBs in adult murine testes have been described previously, such as actin [Russell et al., 1987], sak57 [Tres et al., 1996], protocadherin alpha3 [Johnson et al., 2004], heat shock factor 2 [Alastalo et al., 1998], delta tubulin [Kato et al., 2004], etc. In the present study, we report that Cep55 as well as pericentrin are components of the IBs connecting mouse spermatogonia, spermatocytes, and spermatids. Our immunocytochemical data suggesting that Cep55 as well as pericentrin both are components of germ cell IBs are corroborated by a recent report from Greenbaum et al. [2007], who, by using a proteomic approach to characterize the enriched fraction containing mammalian germ cell IBs, identified several cytokinesis and midbody-related proteins such as MKLP1, MgcRacGAP, Tex14, Septin 2, Septin 7, and Cep55 that are involved in the composition of IBs. In addition, centrosomal protein pericentrin 2 was also identified as a bridge protein [Greenbaum et al., 2007] in the IB-enriched fraction. Here, we showed that Cep55 co-localized with MKLP1 not only in somatic dividing cells in the midbody (Fig. 4) but also co-expressed in germ cell IBs as a double ring structure (Figs. 5 and 6) after the midbody disappeared in spermatogenic IBs. Interestingly, pericentrin, though co-expressed with MKLP1 in germ cell IBs, was not identified localized at the midbody in somatic dividing cells (Fig. 4). Nevertheless, both pericentrin and Cep55 are located in the inner ring of the IBs, forming a double circular structure with MKLP1, of which the IBs outer ring is made up. The ring-like template model for abscission has recently been mentioned in several studies [Mishima et al., 2002; Saint and Somers, 2003; Somers and Saint, 2003; Gromley et al., 2005]. Gromley et al. [2005] noted that a centrosomal protein centriolin begins to accumulate in the midbody as a ring-like

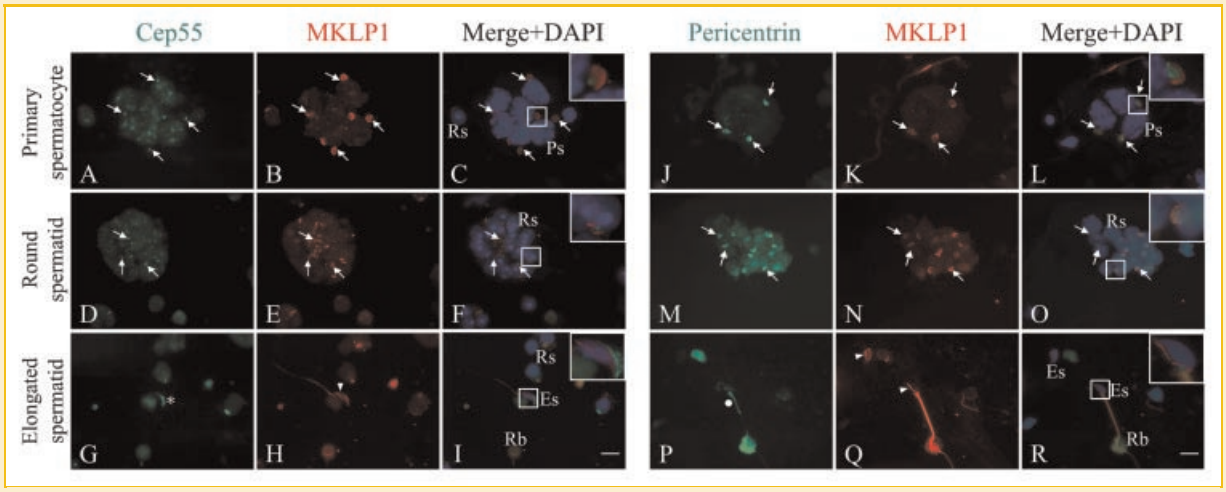

Fig. 6. Immunofluorescent localization of Cep55, MKLP-1, and pericentrin in dissociated cells from adult mouse testis. Double staining with Cep55 (green) and MKLP-1 (red) is depicted in the left column (A–I), and double staining with pericentrin (green) and MKLP-1 (red) is shown in right column (J–R). Arrows (A–F and J–O) indicate double ring structures of intercellular bridges connecting spermatocytes and round spermatids, where Cep55 (insets, C,F) and pericentrin (insets, L,O) are located in the inner layer of the ring structure. In elongated spermatids or sperms, Cep55 was located in the acrosome region (star, G), pericentrin was noted in the neck region and middle piece of the flagellum (dot, P), and MKLP1 was detected in the perinuclear ring (arrowheads, H,Q) and along the whole flagellum. All of three proteins were shed into residual bodies. The nuclei were counterstained with DAPI (blue signal). Ps, spermatocytes; Rs, round spermatids; Es, elongated spermatids; Rb, residual body. Scale bar: 10 μm.

structure not long after furrow formation and recruits both the vesicle targeting and vesicle fusion machinery. The recruitment of centriolin to the midbody ring is dependent on the components of the centralspindlin complex, MKLP1 and MgcRacGAP (male germ cell Rac GTPase-activating protein) [Mishima et al., 2002; Gromley et al., 2005], which also control assembly of the contractile ring [Somers and Saint, 2003]. The diameter of the inner midbody ring maintains constant in size once formed. As constriction proceeds, the outer contractile ring decreases in size until the centralspindlin complexes become concentrated in the midbody [Saint and Somers, 2003; Somers and Saint, 2003]. In contrast to the centriolin model, a double ring model of contractile ring postulates that centralspindlin complexes locate in the inner ring position and activate a cortical equatorial ring of Rho GTPase exchange factor, subsequently leading to the formation and constriction of a contractile ring [Saint and Somers, 2003]. Recently, a novel mammal germ cell IB marker, testis-expressed gene 14 (Tex 14) was identified [Greenbaum et al., 2006, 2009], which was shown to be localized initially to the inner ring in the midbody matrix, then integrated into the outer ring containing centralspindlin as the IB matured [Greenbaum et al., 2007]. Septins 2, 7, and 9 were found to localize to the outer ring of the newly formed bridge but they were not found in mature IBs [Greenbaum et al., 2007]. Interestingly, in this study, we found that both centrosomal proteins Cep55 and pericentrin were persistently present in the inner ring components of IBs without joining the ring structure of MKLP1, which, along with MgcRacGAP exists as an outer ring in IBs, from neonate to adult. Therefore, the spatial distribution patterns and organization of Cep55 and pericentrin in the IBs are markedly different from any known molecules thus far recognized in germ cell IBs.

Recently, several lines of evidence have implicated Cep55 as a regulator required for the completion of cytokinesis [Fabbro et al., 2005; Martinez-Garay et al., 2006; Zhao et al., 2006; Carlton and Martin-Serrano, 2007; Morita et al., 2007; Lee et al., 2008]. Cep55 is concentrated at the centrosome until the onset of prophase when its dissociation from centrosome is triggered by Cdk1/Erk2-dependent phosphorylation [Fabbro et al., 2005]. Following movement to spindle pole regions, mitotic spindle, and the spindle midzone, Cep55 ultimately assembles into the Flemming body, a dense proteinaceous ring that occupies a central position within the midbody [Fabbro et al., 2005; Martinez-Garay et al., 2006; Zhao et al., 2006]. Plk1 subsequently phosphorylates Cep55 at the midbody to drive cells through cytokinesis [Fabbro et al., 2005]. In the absence of Cep55, a series of structural and regulatory factors required for the terminal stages of cytokinesis fail to concentrate at the Flemming body, including Aurora B, MKLP2, Plk1, PRC1, and ECT2 [Zhao et al., 2006], demonstrating that Cep55 is indispensable for midbody structure maintenance. Cep55 also orchestrates the final stage of abscission. During abscission, Cep55 at the midbody recruits two key components of the ESCRT (endosomal sorting complex required for transport) machinery: tumor susceptibility gene 101 (Tsg101), a subunit of the ESCRT-1, and Alix, an ESCRT-associated protein [Carlton and Martin-Serrano, 2007; Morita et al., 2007; Lee et al., 2008]. Depletion of Alix and Tsg101/ESCRT-1 results in cytokinesis failure, rendering an increased proportion of multinucleated cells and/or unusual intercellular connections with arrested midbodies [Carlton and Martin-Serrano, 2007; Morita et al., 2007] which is reminiscent of the defect in cytokinesis that occur with depletion of Cep55 or ectopic expression of phosphorylation-deficient mutant forms of Cep55 [Fabbro et al., 2005]. Although much is known about the role of Cep55 in cell abscission, there are few studies that examine the role of Cep55 in germ cell cytokineis. Our data showing that Cep55 is a novel component of germ cell IBs demonstrate for the first time that Cep55, along with pericentrin, take part in germ cell IB formation after incomplete cytokinesis. The detailed molecular mechanisms of germline IB formation, however,

need further investigation. Both monoclonal and polyclonal antibodies can recognize phosphorylated forms of Cep55. However, in this study, we do not know whether there is any change in the phosphorylation status of Cep55 during spermatogenesis or spermiogenesis.

Although all co-expressed in IBs, Cep55, pericentrin, and MKLP1 displayed different expression patterns in elongated and condensing spermatids. For example, Cep55 immunostaining could be detected in elongated spermatids in the acrosome area surrounding the head, a storage vessel for proteins used in fertilization (Fig. 6G,I). Acrosome-associated Cep55 immunostaining persisted in sperm isolated from cauda epididymis (data not shown), suggesting a possible function for Cep55 in sperm/egg interaction or the acrosome reaction during fertilization. In elongated spermatids, pericentrin was localized to the base of the crescent-shape nucleus (Fig. 6P,R), corresponding to the site of the centrioles, and the middle piece of flagellum, where axoneme is surrounded by a sheath of specialized mitochondria. MKLP1, in addition to its localization at IBs among germ cells, was found in flagella of mouse sperm, suggesting that MKLP1 may be important for basic flagellar functions, including a role in sperm motility. MKLP1 was also detected in the perinuclear ring of the manchette (Fig. 6H,I), which may be involved in the morphological changes of spermatids during spermiogenesis [Kato et al., 2004]. Finally, our results indicated that all three proteins are present in residual bodies in mouse step 15–16 spermatids (Fig. 6G–I,P–R), reflecting a period of centriole reduction in which centrosome-associated proteins were shed in residual bodies [Manandhar et al., 1999; Manandhar et al., 2005].

In conclusion, centrosomal protein Cep55, along with pericentrin, which accumulate in the inner matrix of IBs, may play an essential role in maintaining stable germ cell IBs, and even in the subsequent breakdown of the midbody in mature bridges. It will be important to examine whether other centrosomal or midbody proteins share properties similar to Cep55 and elucidate the detailed molecular mechanisms responsible for germ cell IB formation. Overall, expression profiles of Cep55 during mouse testis development strongly suggest that Cep55 plays a unique and diverse role in spermatogenesis and spermiogenesis.

REFERENCES

Alastalo TP, Lonnstrom M, Leppa S, Kaarniranta K, Pelto-Huikko M, Sistonen L, Parvinen M. 1998. Stage-specific expression and cellular localization of the heat shock factor 2 isoforms in the rat seminiferous epithelium. Exp Cell Res 240:16–27.

Bellve AR, Cavicchia JC, Millette CF, O'Brien DA, Bhatnagar YM, Dym M. 1977. Spermatogenic cells of the prepuberal mouse. Isolation and morphological characterization. J Cell Biol 74:68–85.

Burgos MH, Fawcett DW. 1955. Studies on the fine structure of the mammalian testis. I. Differentiation of the spermatids in the cat (*Felis domestica*). J Biophys Biochem Cytol 1:287–300.

Canman JC, Wells WA. 2004. Rappaport furrows on our minds: The ASCB Cytokinesis Meeting, Burlington, VT, July 22–25, 2004. J Cell Biol 166:943–948.

Carlton JG, Martin-Serrano J. 2007. Parallels between cytokinesis and retroviral budding: A role for the ESCRT machinery. Science 316:1908–1912.

Carmena M, Riparbelli MG, Minestrini G, Tavares AM, Adams R, Callaini G, Glover DM. 1998. Drosophila polo kinase is required for cytokinesis. J Cell Biol 143:659–671.

Chen CH, Lu PJ, Chen YC, Fu SL, Wu KJ, Tsou AP, Lee YC, Lin TC, Hsu SL, Lin WJ, Huang CY, Chou CK, Lee YCG, Lin TCE, Huang CYF. 2007. FLJ10540-elicited cell transformation is through the activation of PI3-kinase/AKT pathway. Oncogene 26:4272–4283.

Chen C-H, Lai J-M, Chou T-Y, Chen C-Y, Su L-J, Lee Y-C, Cheng T-S, Hong Y-R, Chou C-K, Whang-Peng J, Wu Y-C, Huang C-YF. 2009. VEGFA upregulates FLJ10540 and modulates migration and invasion of lung cancer via PI3K/AKT pathway. PLoS One 4:e5052.

Doxsey SJ. 2005. Molecular links between centrosome and midbody. Mol Cell 20:170–172.

Doxsey SJ, Stein P, Evans L, Calarco PD, Kirschner M. 1994. Pericentrin, a highly conserved centrosome protein involved in microtubule organization [see comment]. Cell 76:639–650.

Doxsey S, McCollum D, Theurkauf W. 2005. Centrosomes in cellular regulation. Annu Rev Cell Dev Biol 21:411–434.

Dym M, Fawcett DW. 1971. Further observations on the numbers of spermatogonia, spermatocytes, and spermatids connected by intercellular bridges in the mammalian testis. Biol Reprod 4:195–215.

Eggert US, Mitchison TJ, Field CM. 2006. Animal cytokinesis: From parts list to mechanisms. Annu Rev Biochem 75:543–566.

Fabbro M, Zhou BB, Takahashi M, Sarcevic B, Lal P, Graham ME, Gabrielli BG, Robinson PJ, Nigg EA, Ono Y, Khanna KK. 2005. Cdk1/Erk2- and Plk1-dependent phosphorylation of a centrosome protein, Cep55, is required for its recruitment to midbody and cytokinesis. Dev Cell 9:477–488.

Fawcett DW, Ito S, Slautterback D. 1959. The occurrence of intercellular bridges in groups of cells exhibiting synchronous differentiation. J Biophys Biochem Cytol 5:453–460.

Gemenetzidis E, Bose A, Riaz AM, Chaplin T, Young BD, Ali M, Sugden D, Thurlow JK, Cheong SC, Teo SH, Wan H, Waseem A, Parkinson EK, Fortune F, Teh MT. 2009. FOXM1 upregulation is an early event in human squamous cell carcinoma and it is enhanced by nicotine during malignant transformation. PLoS One 4:e4849.

Glotzer M. 2001. Animal cell cytokinesis. Annu Rev Cell Dev Biol 17:351–386.

Greenbaum MP, Yan W, Wu MH, Lin YN, Agno JE, Sharma M, Braun RE, Rajkovic A, Matzuk MM. 2006. TEX14 is essential for intercellular bridges and fertility in male mice. Proc Natl Acad Sci USA 103:4982–4987.

Greenbaum MP, Ma L, Matzuk MM, Greenbaum MP, Ma L, Matzuk MM. 2007. Conversion of midbodies into germ cell intercellular bridges. Dev Biol 305:389–396.

Greenbaum MP, Iwamori N, Agno JE, Matzuk MM. 2009. Mouse TEX14 is required for embryonic germ cell intercellular bridges but not female fertility. Biol Reprod 80:449–457.

Gromley A, Yeaman C, Rosa J, Redick S, Chen CT, Mirabelle S, Guha M, Sillibourne J, Doxsey SJ. 2005. Centriolin anchoring of exocyst and SNARE complexes at the midbody is required for secretory-vesicle-mediated abscission. Cell 123:75–87.

Guo GQ, Zheng GC. 2004. Hypotheses for the functions of intercellular bridges in male germ cell development and its cellular mechanisms. J Theor Biol 229:139–146.

Johnson KJ, Zecevic A, Kwon EJ. 2004. Protocadherin alpha3 acts at sites distinct from classic cadherins in rat testis and sperm. Biol Reprod 70:303–312.

Kato A, Nagata Y, Todokoro K. 2004. Delta-tubulin is a component of intercellular bridges and both the early and mature perinuclear rings during spermatogenesis. Dev Biol 269:196–205.

Lee HH, Elia N, Ghirlando R, Lippincott-Schwartz J, Hurley JH. 2008. Midbody targeting of the ESCRT machinery by a noncanonical coiled coil in CEP55. Science 322:576–580.

Manandhar G, Simerly C, Salisbury JL, Schatten G. 1999. Centriole and centrin degeneration during mouse spermiogenesis. Cell Motil Cytoskeleton 43:137–144.

Manandhar G, Schatten H, Sutovsky P. 2005. Centrosome reduction during gametogenesis and its significance. Biol Reprod 72:2–13.

Martinez-Garay I, Rustom A, Gerdes HH, Kutsche K. 2006. The novel centrosomal associated protein CEP55 is present in the spindle midzone and the midbody. Genomics 87:243–253.

Minestrini G, Mathe E, Glover DM. 2002. Domains of the Pavarotti kinesin-like protein that direct its subcellular distribution: Effects of mislocalisation on the tubulin and actin cytoskeleton during Drosophila oogenesis. J Cell Sci 115:725–736.

Mishima M, Kaitna S, Glotzer M. 2002. Central spindle assembly and cytokinesis require a kinesin-like protein/RhoGAP complex with microtubule bundling activity [see comment]. Dev Cell 2:41–54.

Montoya M. 2007. An ESCRT for daughters. Nat Struct Mol Biol 14: 579.

Morita E, Sandrin V, Chung HY, Morham SG, Gygi SP, Rodesch CK, Sundquist WI. 2007. Human ESCRT and ALIX proteins interact with proteins of the midbody and function in cytokinesis. EMBO J 26:4215–4227.

Mullins JM, Biesele JJ. 1973. Cytokinetic activities in a human cell line: The midbody and intercellular bridge. Tissue Cell 5:47–61.

Mullins JM, Biesele JJ. 1977. Terminal phase of cytokinesis in D-98s cells. J Cell Biol 73:672–684.

Pohl C, Jentsch S. 2008. Final stages of cytokinesis and midbody ring formation are controlled by BRUCE. Cell 132:832–845.

Rattner JB. 1992. Mapping the mammalian intercellular bridge. Cell Motil Cytoskeleton 23:231–235.

Robinson DN, Cooley L. 1996. Stable intercellular bridges in development: The cytoskeleton lining the tunnel. Trends Cell Biol 6:474–479.

Robinson DN, Cant K, Cooley L. 1994. Morphogenesis of Drosophila ovarian ring canals. Development 120:2015–2025.

Russell LD, Vogl AW, Weber JE. 1987. Actin localization in male germ cell intercellular bridges in the rat and ground squirrel and disruption of bridges by cytochalasin D. Am J Anat 180:25–40.

Saint R, Somers WG. 2003. Animal cell division: A fellowship of the double ring? J Cell Sci 116:4277–4281.

Sakai M, Shimokawa T, Kobayashi T, Matsushima S, Yamada Y, Nakamura Y, Furukawa Y. 2006. Elevated expression of C10orf3 (chromosome 10 open reading frame 3) is involved in the growth of human colon tumor. Oncogene 25:480–486.

Somers WG, Saint R. 2003. A RhoGEF and Rho family GTPase-activating protein complex links the contractile ring to cortical microtubules at the onset of cytokinesis. Dev Cell 4:29–39.

Terasima T, Tolmach LJ. 1963. Growth and nucleic acid synthesis in synchronously dividing populations of HeLa cells. Exp Cell Res 30:344–362.

Tobey RA, Anderson EC, Petersen DF. 1967. Properties of mitotic cells prepared by mechanically shaking monolayer cultures of Chinese hamster cells. J Cell Physiol 70:63–68.

Tres LL, Rivkin E, Kierszenbaum AL. 1996. Sak 57, an intermediate filament keratin present in intercellular bridges of rat primary spermatocytes. Mol Reprod Dev 45:93–105.

Weber JE, Russell LD. 1987. A study of intercellular bridges during spermatogenesis in the rat. Am J Anat 180:1–24.

Zhao WM, Seki A, Fang G. 2006. Cep55, a microtubule-bundling protein, associates with centralspindlin to control the midbody integrity and cell abscission during cytokinesis. Mol Biol Cell 17:3881–3896.